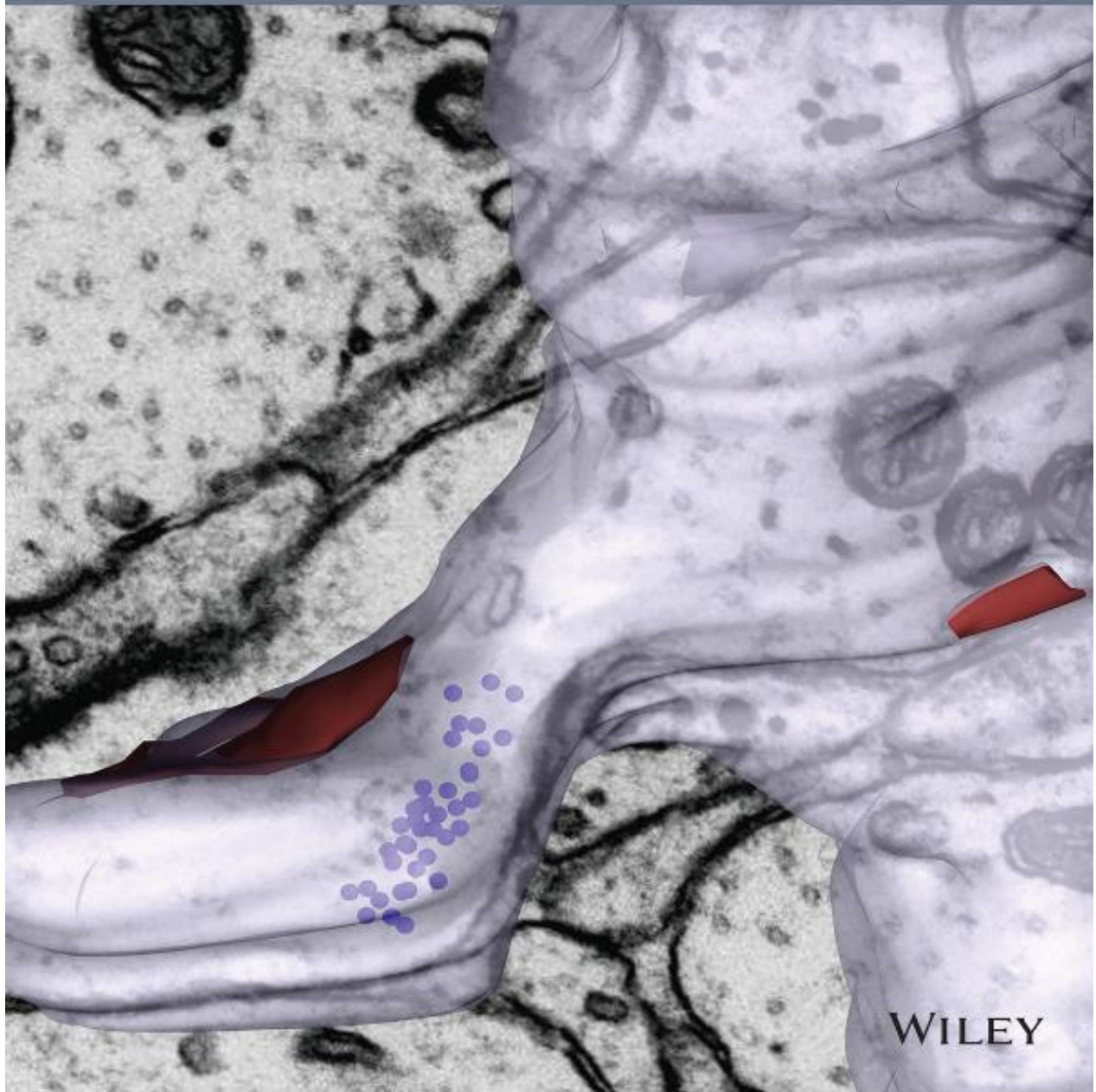


VOLUME 28, NUMBER 6, 2018


Hippocampus



WILEY

RESEARCH ARTICLE

Shifting patterns of polyribosome accumulation at synapses over the course of hippocampal long-term potentiation

Linnaea E. Ostroff¹  | Deborah J. Watson² | Guan Cao² |
Patrick H. Parker² | Heather Smith² | Kristen M. Harris²

¹Department of Physiology and Neurobiology, University of Connecticut, Storrs, Connecticut 06269

²Department of Neuroscience, Center for Learning and Memory, Institute for Neuroscience, University of Texas at Austin, Austin, Texas 78731

Correspondence

Linnaea E. Ostroff, Department of Physiology and Neurobiology, University of Connecticut, Storrs, CT 06269

Email: linnaea.ostroff@uconn.edu

Kristen M. Harris, Department of Neuroscience, Center for Learning and Memory, Institute for Neuroscience, University of Texas at Austin, Austin, TX 78731

Email: kharris@mail.clm.utexas.edu

Present addresses

Deborah J. Watson, QPS, LLC, in vivo ADME, Newark, DE 19702

Heather Smith, Department of Surgery, Section of Neurosurgery, University of Chicago, Chicago, IL 60637

Funding information

National Institute of Mental Health, Grant/Award Number: MH095980, MH096459; National Institute of Neurological Disorders and Stroke, Grant/Award Number: NS074644, NS201184

Abstract

Hippocampal long-term potentiation (LTP) is a cellular memory mechanism. For LTP to endure, new protein synthesis is required immediately after induction and some of these proteins must be delivered to specific, presumably potentiated, synapses. Local synthesis in dendrites could rapidly provide new proteins to synapses, but the spatial distribution of translation following induction of LTP is not known. Here, we quantified polyribosomes, the sites of local protein synthesis, in CA1 stratum radiatum dendrites and spines from postnatal day 15 rats. Hippocampal slices were rapidly fixed at 5, 30, or 120 min after LTP induction by theta-burst stimulation (TBS). Dendrites were reconstructed through serial section electron microscopy from comparable regions near the TBS or control electrodes in the same slice, and in unstimulated hippocampus that was perfusion-fixed *in vivo*. At 5 min after induction of LTP, polyribosomes were elevated in dendritic shafts and spines, especially near spine bases and in spine heads. At 30 min, polyribosomes remained elevated only in spine bases. At 120 min, both spine bases and spine necks had elevated polyribosomes. Polyribosomes accumulated in spines with larger synapses at 5 and 30 min, but not at 120 min. Small spines, meanwhile, proliferated dramatically by 120 min, but these largely lacked polyribosomes. The number of ribosomes per polyribosome is variable and may reflect differences in translation regulation. In dendritic spines, but not shafts, there were fewer ribosomes per polyribosome in the slice conditions relative to *in vivo*, but this recovered transiently in the 5 min LTP condition. Overall, our data show that LTP induces a rapid, transient upregulation of large polyribosomes in larger spines, and a persistent upregulation of small polyribosomes in the bases and necks of small spines. This is consistent with local translation supporting enlargement of potentiated synapses within minutes of LTP induction.

KEYWORDS

local translation, long-term potentiation, serial section electron microscopy, structural plasticity

1 | INTRODUCTION

Like long-term memory, long-term potentiation (LTP) consists of two fundamental phases: an early, protein synthesis-independent phase lasting minutes to hours, and a persistent, protein synthesis-dependent late phase (reviewed in Abraham & Williams, 2008; Alberini, 2008; Davis & Squire, 1984; Kelleher, Govindarajan, & Tonegawa, 2004). In the hippocampus, inhibition of protein synthesis during or immediately after induction of LTP results in an early phase of LTP that decays to baseline within a couple hours (Frey, Krug, Reymann, & Matthies,

1988; Krug, Lössner, & Ott, 1984; Stanton & Sarvey, 1984). This decay is avoided if translation inhibitors are applied after a delay of 10–60 min (Costa-Mattioli et al., 2007; Frey & Morris, 1997; Otani, Marshall, Tate, Goddard, & Abraham, 1989), demonstrating that the translation required for late LTP actually occurred much earlier. Consistent with this interpretation, a recent study examined ribosome-bound mRNAs after hippocampal LTP induction and found substantial shifts in the complement of transcripts over the first two hours (Chen et al., 2017).

Structural plasticity also occurs during the first 2 hr after the induction of LTP. In developing and juvenile hippocampus, dendritic spines

can enlarge within 5 min of LTP induction, and new spines can form within 30–120 min (Engert & Bonhoeffer, 1999; Matsuzaki Honkura, Ellis-Davies, & Kasai, 2004; Segal, 2016; Watson et al., 2016). New protein synthesis is necessary to stabilize spine enlargement induced by LTP or glutamate stimulation, and hence supports a direct role for protein synthesis in synapse remodeling during the consolidation of early LTP to late LTP (Fifkova Anderson, Young, & Van Harreveld, 1982; Tanaka et al., 2008). Local protein synthesis occurs in dendrites, where it may serve as a source of new proteins during synaptic plasticity (Holt & Schuman, 2013; Martin & Ephrussi, 2009). In hippocampal slices, local application of a protein synthesis inhibitor to CA1 dendrites during induction blocks late LTP, demonstrating that at least some of the necessary translation must occur in dendrites (Bradshaw, Emptage, & Bliss, 2003). Furthermore, several studies have shown that translation-dependent late LTP can be induced in CA1 dendrites that have been disconnected from the soma (Cracco, Serrano, Moskowitz, Bergold, & Sacktor, 2005; Huang & Kandel, 2005; Kang & Schuman, 1996; Vickers, Dickson, & Wyllie, 2005). More than 2,500 mRNAs have been identified in CA1 dendrites (Cajigas et al., 2012; Poon, Choi, Jamieson, Geschwind, & Martin, 2006; Zhong, Zhang, & Bloch, 2006), including the transcript of the synaptic molecule CaMKII α , whose dendritic targeting sequence is necessary for both LTP and long-term memory (Miller et al., 2002). Neurons possess an extensive repertoire of intracellular trafficking mechanisms that can deliver proteins from the soma to distal processes (Hirokawa & Takemura, 2005; Maeder, Shen, & Hoogenraad, 2014); yet local translation is necessary, and possibly sufficient, to support LTP.

As a protein targeting mechanism, local translation is especially valuable when proteins are needed more quickly than they can be transported, or when their availability must be spatially restricted. Either or both of these conditions could explain the role of local translation in LTP. In rat CA1 stratum radiatum, synapses on higher order dendritic branches are located ~200–400 μm or more from the soma (Routh, Johnston, Harris, & Chitwood, 2009). Dendritic transport rates of up to 1 $\mu\text{m}/\text{s}$ have been reported in cultured hippocampal neurons over short distances (Kapitein et al., 2010; McNamara, Grigston, VanDongen, & VanDongen, 2004), so even if these high velocities were sustained it would take at least 5 min for pre-existing proteins to reach the average synapse from the soma. Local translation of dendritic mRNA could supply proteins more quickly and potentially prevent proximal synapses from accumulating proteins at the expense of distal synapses. If it is regulated on a fine enough spatial scale, local translation could also allow new proteins to be restricted to individual synapses, thus supporting synapse specificity during LTP. Consistent with this possibility, both mRNA (Kao, Aldridge, Weiler, & Greenough, 2010; Tiruchinapalli et al., 2003) and polyribosomes (Ostroff, Fiala, Allwardt, & Harris, 2002) are found in the heads of dendritic spines, and we have previously found that polyribosomes accumulate in spines with enlarged synapses two hours after LTP induction by tetanic stimulation (Ostroff et al., 2002).

On the other hand, there is evidence that new LTP-related proteins can be shared among synapses. Experiments using two stimulation pathways onto the same dendrites have found that within an hour

of inducing LTP on one pathway, late LTP can be induced on the other pathway by subthreshold stimulation or in the presence of a protein synthesis inhibitor (Frey & Morris, 1997; Govindarajan, Israely, Huang, & Tonegawa, 2011). This finding confirms that the essential proteins are translated in the first minutes of LTP and suggests that making these proteins available to activated synapses is sufficient for LTP. Furthermore, these experiments suggest that synapse-specific regulation of translation may be unnecessary. In our previous study, we found that the increase in polyribosomes in spines was balanced by a decrease in dendritic shafts, which would be consistent with spine polyribosomes being drawn from a general pool in the dendrite (Ostroff et al., 2002). Since this observation was made at 2 hr after induction of LTP by tetanic stimulation, new proteins, and RNA may have arrived from the soma, so those polyribosomes might not have reflected the critical translation that was induced during the first few minutes.

Here, we investigated the spatial and temporal dynamics of local translation during the early phase of LTP when translation that supports the later phases occurs. In addition, we used multiple trains of theta-burst stimulation (TBS) to saturate LTP. We quantified the distribution of polyribosomes in CA1 dendrites at 5, 30, and 120 min after LTP induction. We hypothesized that if local translation is regulated in a synapse-specific manner, polyribosomes would accumulate especially in large spines thought to undergo induction of LTP. On the other hand, if local translation serves as a rapid source of proteins for the dendritic compartment, there might be a nonspecific increase throughout the dendrite, perhaps followed by more specific localization in spines. This study was performed in juvenile animals, just after the developmental onset of late-phase hippocampal LTP (Cao & Harris, 2012), in part to minimize the background of experience-driven plasticity. We previously analyzed the dendritic spines in this material and found that LTP induced synaptogenesis and a net increase in synapses along dendrites (Watson et al., 2016). This developmental finding contrasts with the structural synaptic scaling that occurs in hippocampal slices from adult rats (Bourne & Harris, 2011). Thus, we were able to observe how polyribosome distribution related to LTP-induced synaptogenesis as well.

2 | MATERIALS AND METHODS

Analysis was performed on an existing data set, and complete methodological details are published elsewhere (Watson et al., 2016). All animal use procedures were approved by the Institutional Animal Care and Use Committee at the University of Texas at Austin and complied with the NIH requirements for the humane use of laboratory rats.

2.1 | Slice electrophysiology

Hippocampal slices were prepared from postnatal day 15 (P15) male Long-Evans rats. Animals were decapitated, and their left hippocampi were dissected free and cut at 400 μm in the transverse plane on a tissue chopper (Stoelting Co., Wood Dale, IL). Slices were cut at room temperature and transferred within 5 min of decapitation to a 34°C static-pool interface chamber in ACSF (117 mM NaCl, 5.3 mM KCl,

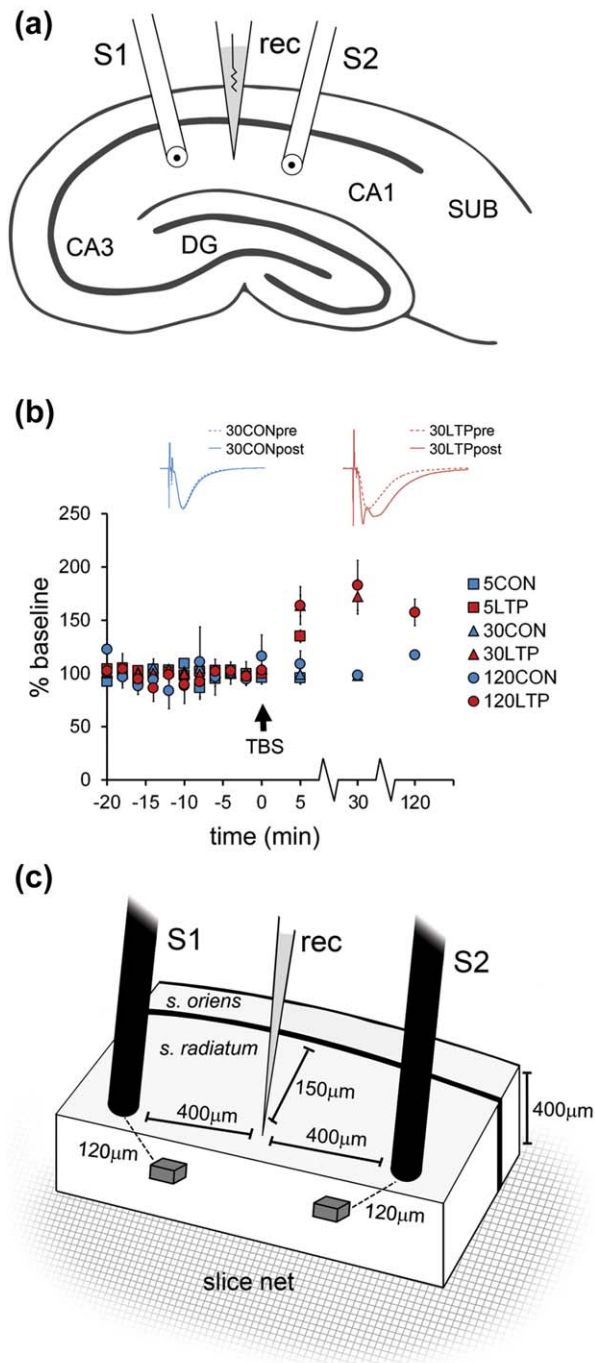


FIGURE 1 Experimental design and physiology outcomes. (a) Drawing of hippocampal slice showing placement of recording pipet (rec) in CA1 between two stimulating electrodes (S1 and S2). DG, dentate gyrus; SUB, subiculum. (b) Average fEPSP slope as % of pre-TBS baseline for all three time points. For clarity, only the post-TBS time points immediately before each fixation time point are shown. Inset: average waveforms from the 30 min time point. (c) Drawing of area around electrodes showing location of sampling for electron microscopy (gray cubes) [Color figure can be viewed at wileyonlinelibrary.com]

2.5 mM CaCl₂, 1.3 mM MgSO₄, 1 mM NaH₂PO₄, 26 mM NaHCO₃, 10 mM glucose, and 95% O₂/5% CO₂ at pH 7.4). After 1 hr of recovery, two concentric bipolar stimulating electrodes (100 μm outer

diameter; FHC, Bowdoin, ME) were placed 600–800 μm apart in CA1 stratum radiatum with a 120 mM NaCl-filled glass recording pipette halfway between them, ~150–200 μm from the cell body layer (Figure 1a). Responses were amplified, filtered at 2 kHz, and recorded using customized IGOR software (WaveMetrics Inc., Lake Oswego, OR). An initial input–output curve was used to set the stimulus intensity of each electrode to 75% of the population spike threshold for the remainder of the experiment. Test pulses were given every 120 s, with a 30 s interval between the two electrodes. Responses were measured as the maximal slope over a 400 μs time frame of the initial field excitatory postsynaptic potential (fEPSP). After a minimum of 40 min of stable baseline recordings, LTP was induced at one of the two inputs by TBS, consisting of eight trains at 30 s intervals of 10 bursts at 5 Hz of 4,200 μs biphasic pulses at 100 Hz. Test pulse stimulation resumed for the remainder of the experiment. The TBS and control electrodes were counterbalanced between the subicular and CA3 sides of the slices.

2.2 | Fixation

Slices were fixed 5 min ($n = 2$), 30 min ($n = 3$), or 120 min ($n = 2$) after TBS by transferring them quickly, without removing them from their supporting net, into mixed aldehydes (6% glutaraldehyde, 2% paraformaldehyde, 2 mM CaCl₂, and 4 mM MgCl₂ in 0.1 M cacodylate buffer at pH 7.4) and microwaving them for 10–25 s to a final temperature of <35 °C. Slices were left in fixative at room temperature overnight, then rinsed in buffer and embedded in agarose. The area of CA1 containing the electrode tracks was dissected out and sectioned at 70 μm perpendicular to the slice plane on a vibrating slicer (Leica Microsystems). Sections containing the two electrode tracks plus the two sections on either side were selected for further processing.

For perfusion fixation, 15-day-old male Long-Evans rats ($n = 2$) were deeply anesthetized with pentobarbital (80 mg/kg) and perfused transcardially with mixed aldehydes (2.5% glutaraldehyde, 2% paraformaldehyde, 2 mM CaCl₂, and 4 mM MgSO₄ in 0.1 M cacodylate buffer at pH 7.4). Brains were removed >1 hr after perfusion and kept in slice fixative (with 6% glutaraldehyde) overnight at room temperature. After rinsing in buffer, brains were sectioned at 400 μm and the left hippocampi were dissected and vibra-sliced in the same manner as the slices.

2.3 | Tissue processing and imaging

Tissue sections were processed for electron microscopy (EM) using a laboratory microwave (Ted Pella, Inc.). Sections were post-fixed under vacuum at 150 W in chilled (19 °C) reduced osmium (1% OsO₄/2% KFeCN in 0.1 M cacodylate) for 4 min total, and then in chilled 1% OsO₄ in 0.1 M cacodylate for 4 min total. After rinsing, sections were dehydrated at 250 W through an ascending series of ethanol dilutions, with each containing 1% uranyl acetate, for 40 s. The ethanol was gradually replaced with acetone and the sections were infiltrated under vacuum at 350 W with a series of acetone dilutions (50%–100%) of LX-112 (Ladd Research Industries, Williston, VT) for 12 min total. The sections were embedded in flat coffin molds (Structure Probe Inc., West Chester, PA) and cured at 60 °C in a conventional oven for 48 hr.

Coded resin blocks containing the tissue sections adjacent to the stimulating electrode indentations (~50 μm deep from the air surface) were used to obtain serial sections at the LTP and control sites. Sectioning trapezoids were positioned 50–80 μm lateral to the indentations and 125–150 μm deep, for a diagonal distance of ~135–170 μm from the center of the electrode. At this location the narrow P15 dendritic arbor was not likely to have been stimulated directly. In addition, this location was at a depth of 175–200 μm from the air surface of the slice, an area where dendrites, synapses, and astroglia had the healthiest appearance. Serial sections were cut at 45 nm thickness from each trapezoid on an Ultracut T microtome (Leica Microsystems) and picked up on Pioloform-coated Synpatek slot grids (Electron Microscopy Sciences, Hatfield, PA). An average of 163 ± 9.7 serial sections (range: 120–218) from each sample was imaged on a JEOL 1230 electron microscope with a Gatan digital camera at 4,000–10,000 \times magnification.

2.4 | Reconstruction and analysis

All image analyses, including alignment, calibration, reconstruction, and measurements, were done using Reconstruct software (available at <http://synapseweb.clm.utexas.edu>; Fiala, 2005) with the experimenter blind to condition. Three-dimensional renderings were prepared using 3ds Max software (Autodesk, Inc., San Rafael, CA). We analyzed small caliber spiny dendrites that were in cross section on the central section of each series and whose protrusions were contained within the image volume. Microtubule number was used as a proxy for dendrite caliber because over the length of a dendrite it is well correlated with dendrite diameter and cross-sectional area, but these more traditional measurements of caliber are much more variable between sections (Fiala et al., 2003; Ostroff, Cain, Bedont, Monfils, & LeDoux, 2010). The analyzed dendrites contained 5–25 microtubules (average 12.0 ± 0.3) and represent calibers across which there is no correlation between caliber and spine density or average synapse area. Unbiased frequency measures were taken by including the first complete by including the first complete protrusion (defined as a spine, shaft synapse, or filopodium) or synapse, and excluding the last protrusion or synapse along each dendritic segment. Variability between segment lengths was minimized by subdividing very long segments (Fiala & Harris, 2001). The final analyzed data set consisted of 153 dendritic segments with a total length of 612 μm (average 4.00 ± 0.07 , range 2.2–6.6 μm).

2.5 | Statistics

ANOVAs were used to compare means between the control and LTP conditions separately for each time point, and to compare the control condition of each time point to the perfused condition. For comparisons between LTP and control, a factorial ANOVA was used to test for interactions between LTP and experiment. Significant interactions were found in two instances, but in both cases the interaction resulted from a difference in the magnitude, not the direction, of the LTP effect between experiments. For comparisons between control and perfused, hierarchical nested ANOVAs (hnANOVAs) with experiment nested in

condition were used to account for inter-experiment variability. When LTP effects were found for more than one time point, hnANOVAs were used to compare the three LTP conditions to each other, followed by a post hoc Bonferroni test. Because ribosome counts followed a log-normal distribution, data were log transformed before ANOVAs were run. STATISTICA software (StatSoft, Tulsa, OK) was used for all analyses. Outcomes are given in figure legends or appropriate results sections with statistical significance set at $p < .05$.

3 | RESULTS

To compare LTP with control stimulation, we used an acute, within-slice experimental design (Figure 1a). Two stimulating electrodes were placed 600–800 μm apart in CA1 stratum radiatum with a recording pipette halfway between, allowing responses to be monitored from two separate populations in the same slice. After collection of baseline responses from both electrodes, TBS was delivered at one electrode and slices were fixed 5, 30, or 120 min later (Figure 1b). EM image volumes were sampled from an area of healthy tissue below and to the side of each stimulating electrode, ~120 μm from the center of the electrode (Figure 1c). Healthy tissue was assessed by its morphological resemblance to perfused tissue and was found near the center of the slice. In contrast, tissue near the slice surfaces showed signs of stress, such as hypertrophied organelles and retracted astrocytic processes. To assess the effects of slice preparation and in vitro conditions, tissue was also sampled from the same region in age-matched, perfusion-fixed animals. Segments of spiny dendrites, including spines and synapses, were reconstructed in three dimensions. Detailed measurements and analysis of spine and synapse morphology have been published elsewhere (Watson et al., 2016).

3.1 | Upregulation of dendritic polyribosomes occurred transiently after LTP induction

First, we determined whether the dendritic and synaptic distribution of local protein synthesis, as indicated by polyribosomes, was dynamically responsive over time after the induction of LTP. To compare numbers of dendritic polyribosomes between experimental groups, we quantified the number of polyribosomes per unit length of dendrite. Polyribosomes were identified by their distinctive morphology, consisting of individual ribosomes, which are ~10–25 nm in diameter with dark centers and irregular gray edges, typically arranged in rosettes, spirals, or staggered lines (Ostroff et al., 2002; Peters, Palay, & Webster, 1991; Steward & Levy, 1982; Warner, Rich, & Hall, 1962). We defined polyribosomes as consisting of at least three ribosomes to minimize ambiguity in identifications. Although rough endoplasmic reticulum was observed in large apical dendrites and branch points, it was not readily identified in spines or the small dendrites of this data set, and we therefore restricted our analyses to free polyribosomes. Dendritic protrusions were classified as spines if they carried at least one synapse, and protrusions without synapses were classified as filopodia (Watson et al., 2016).

Polyribosomes occurred in dendritic shafts (Figure 2a) and spines (Figure 2b) in all experimental groups. Polyribosome frequencies were

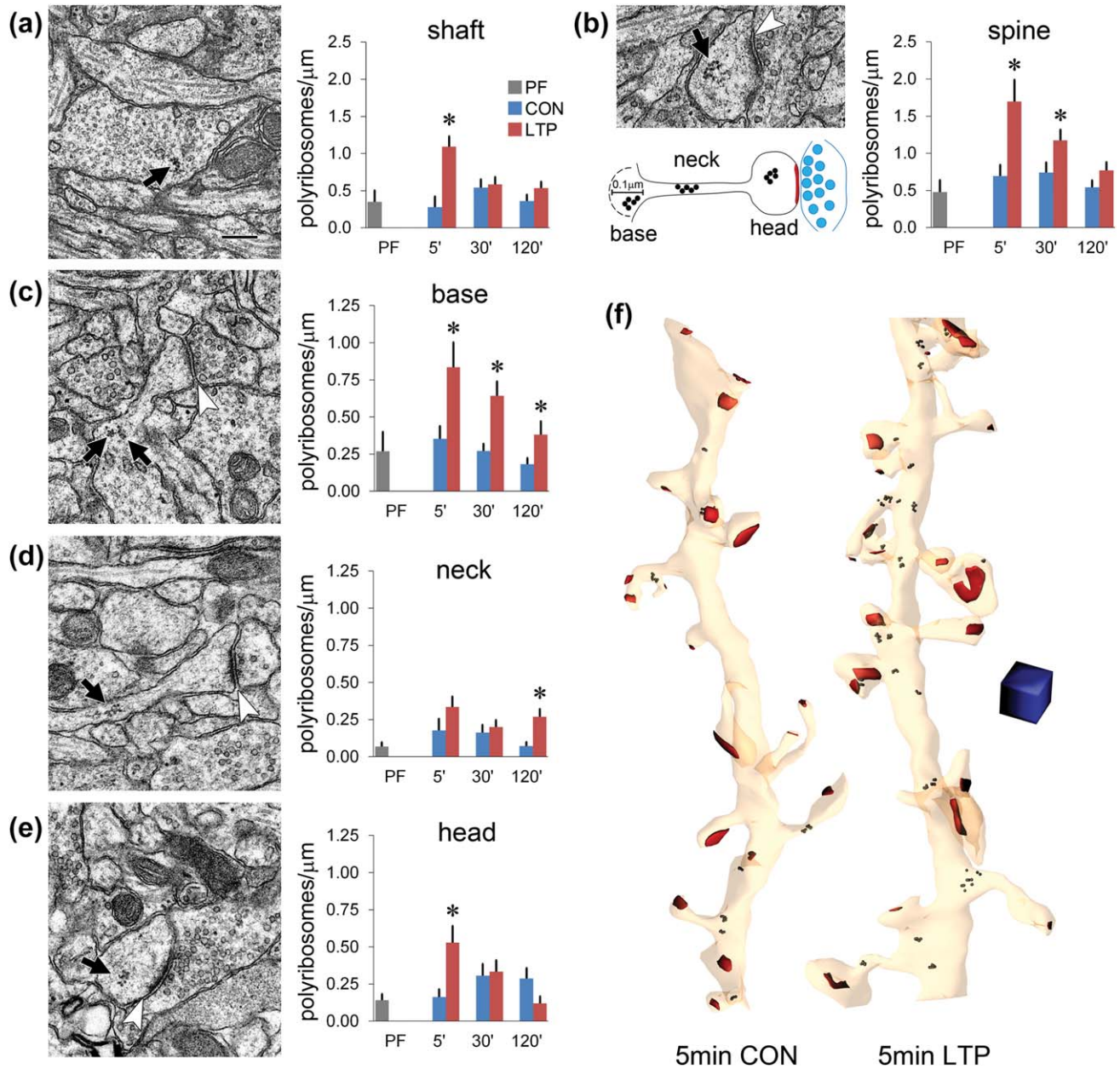


FIGURE 2 Transient global elevation of polyribosomes in dendritic shafts and spines was followed by sustained elevation of polyribosomes in spine bases and necks during LTP. (a) Left: EMs of a polyribosome (arrow) in a dendritic shaft from the 120 min LTP condition. Right: There were more polyribosomes in dendritic shafts in the 5 min LTP condition ($F_{(1, 37)} = 14.12, p = .00059$; LTP \times experiment interaction $F_{(1, 35)} = 12.23, p = .0013$). (b) Top left: EM of a polyribosome (arrow) in the head of a dendritic spine receiving a synapse (arrowhead) from the 120 min LTP condition. Bottom left: Diagram of locations of polyribosomes (black) within a dendritic spine. The PSD (red) and presynaptic vesicles (blue) are also shown. Right: There were more polyribosomes in dendritic spines with LTP at 5 min ($F_{(1, 37)} = 9.20, p = .0044$) and 30 min ($F_{(1, 49)} = 4.77, p = .034$). (c–e) Left: EMs of polyribosomes (arrows) in a spine base (c), neck (d), and head (e) from the 120 min LTP (c) and 120 min control (d, e) conditions; arrowheads indicate synapses. Right: There were more polyribosomes in the base of dendritic spines (c) 5 min ($F_{(1, 37)} = 6.41, p = .016$), 30 min ($F_{(1, 49)} = 10.49, p = .0022$), and 120 min ($F_{(1, 44)} = 4.39, p = .042$) after LTP induction. There were no differences among the three LTP groups ($F_{(2, 63)} = 3.10, p = .052$). There were more polyribosomes in spine necks (d) at 120 min ($F_{(1, 44)} = 12.25, p = .0011$) and in spine heads (e) at 5 min ($F_{(1, 37)} = 8.78, p = .0053$). (f) Reconstructed dendrites from the 5 min experiment (left, control; right, LTP) showing polyribosomes (black) and synapses (red). Effects at $p < .05$: * control versus LTP; # control versus perfused. Scale in a–e = 250 nm, blue cube in f = 500 nm/side [Color figure can be viewed at wileyonlinelibrary.com]

not significantly different at any times between control slices and perfusion-fixed hippocampus in the dendritic shafts (Figure 2a) or spines (Figure 2b). In dendritic shafts, there were more polyribosomes at 5 min, but not at 30 or 120 min after induction of LTP (Figure 2a). In

dendritic spines, there were more polyribosomes at 5 and 30 min, but the elevation did not reach statistical significance at 120 min after induction of LTP (Figure 2b). To quantify the distribution within spines (Figure 2b, diagram), polyribosomes were classified by location in the

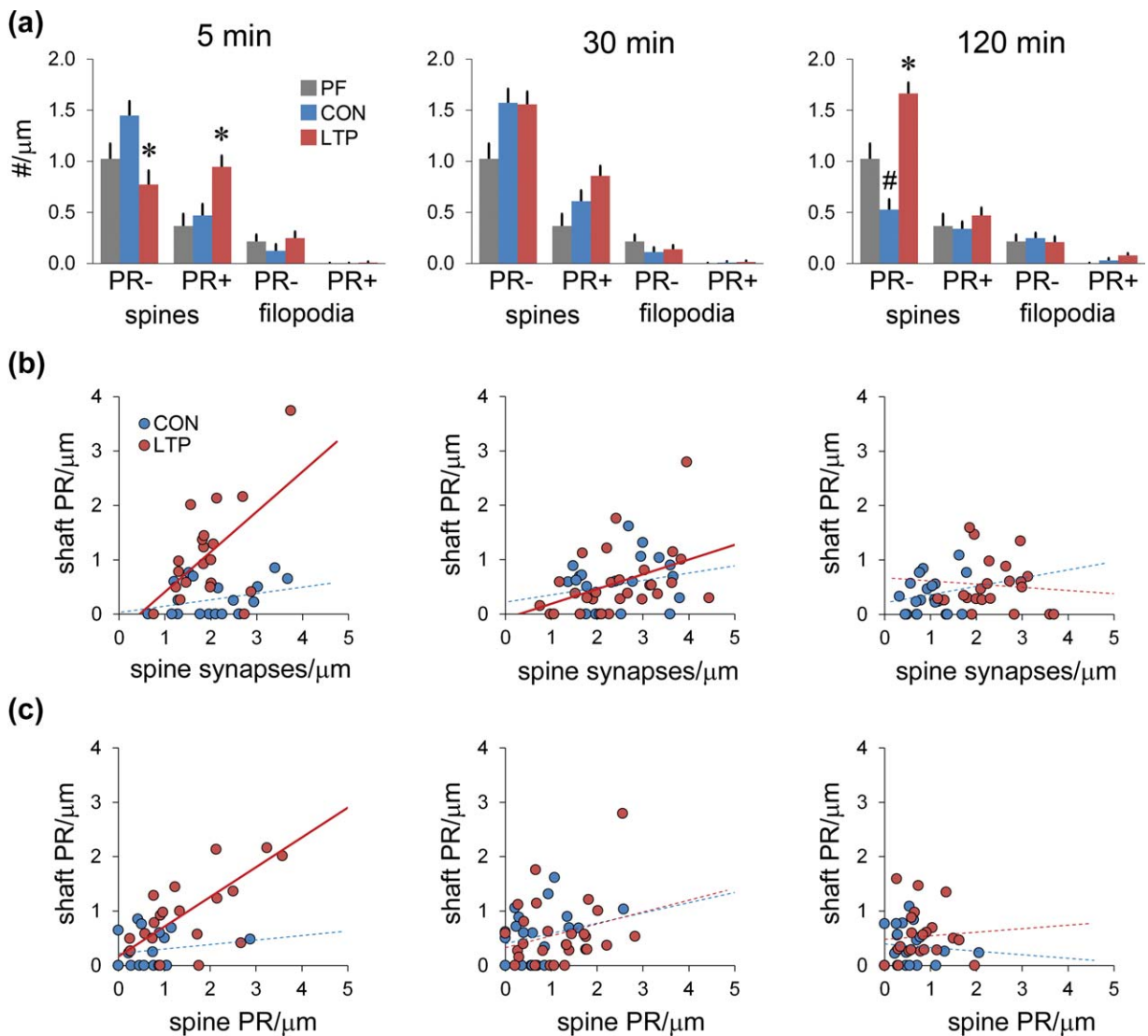


FIGURE 3 Spine frequency with respect to spine and shaft polyribosomes over the course of LTP. (a) At 5 min, there were fewer spines without polyribosomes ($F_{(1, 37)} = 10.50, p = .0025$; LTP \times experiment interaction $F_{(1, 35)} = 11.01, p = .0021$) and more with polyribosomes ($F_{(1, 37)} = 8.86, p = .0051$) in the LTP versus control conditions. At 120 min, there were fewer spines without polyribosomes in the LTP condition versus the control ($F_{(1, 44)} = 58.12, p < .00001$) or perfusion-fixed ($F_{(1, 37)} = 12.43, p = .0012$). There were 123 filopodia across all conditions and just 13 had polyribosomes; all were in the control or LTP conditions at 120 min and three emerged from spine heads while the other 10 emerged directly from the dendritic shafts. (b) The frequency of polyribosomes in dendritic shafts and spines were significantly correlated in the LTP condition at both 5 min (solid lines; Pearson's $r = .56, p = .0097$) and 30 min ($r = .43, p = .022$), but not in other conditions. (c) Shaft and spine polyribosome frequency were significantly correlated in the 5 min LTP condition only ($r = .79, p = .000030$) only. Effects at $p < .05$: * control versus LTP; # control versus perfused. Dashed lines in b, c indicate nonsignificant correlations [Color figure can be viewed at wileyonlinelibrary.com]

base (defined as being within $0.1 \mu\text{m}$ of the spine origin, Figure 2c), spine neck (Figure 2d), or spine head (Figure 2e). Reconstructions of representative dendrites illustrate differences in polyribosome distribution between the control and LTP conditions at 5 min (Figure 2f). At 5 min after induction of LTP, polyribosomes were markedly elevated in spine bases and heads, but the subtle increase in spine necks did not reach statistical significance. At 30 min after induction of LTP, polyribosomes remained elevated only at the spine bases, while at 120 min, polyribosomes were elevated in both spine bases and necks. There was a nonsignificant decrease ($p = .056$) in polyribosomes in spine heads at 120 min, which explains the lack of an overall effect in spines despite

increases in both bases and necks (compare graph in Figure 2b, 120'). Thus, the overall pattern was an early increase in polyribosomes that returned to baseline but persisted longer in the spines than in the dendritic shafts, especially in spine bases and necks.

3.2 | Upregulation of polyribosomes was associated with synapses on existing spines and not filopodia or new spines

Previously, we found that LTP produced new spines and reversed spine loss that occurred in the control slice conditions by 120 min (Watson

et al., 2016). In addition, this prior work showed a subtle increase in filopodia in both LTP and control conditions relative to in vivo perfused at the 120 min time point. Filopodia were defined as nonsynaptic protrusions from the dendritic shaft or a spine head. Therefore, we wanted to know whether the upregulation in polyribosomes occurred in new spines or filopodia, or in existing spines that would have been the only ones present at the time when LTP was induced.

At 5 min, the increase in polyribosome-containing spines (PR+) was perfectly matched by the decrease in spines without polyribosome (PR-, Figure 3a). At 30 min, the parallel increases in PR- and PR+ spines, in both control and LTP slice conditions relative to the perfusion-fixed condition, did not reach statistical significance. At 120 min, spine density in the control condition dropped below that of the perfusion-fixed hippocampus but was dramatically increased after LTP; both effects were specific to spines without polyribosomes. These findings suggest that the transient increases in polyribosomes occurred specifically in existing dendritic spines.

No filopodia had polyribosomes in the perfusion-fixed hippocampus and only 13 out of the 123 filopodia (~11%) contained polyribosomes in the slices (Figure 3a). Filopodia are thin and lack bulbous heads, raising the question of whether they would have sufficient space for polyribosomes. Of the polyribosomes that were found in filopodia, 7 (~50%) were located along the length of the filopodium. Thus, protrusion volume did not explain the absence of polyribosomes in filopodia; rather, polyribosomes localized preferentially to spines with synapses.

Upregulation of shaft polyribosomes could reflect LTP-related proteins made generally available to synapses in activated dendritic segments (Govindarajan et al., 2011), or an upregulation of housekeeping proteins throughout the dendrites. In the former case, shaft polyribosomes should be associated with spine synapses and polyribosomes. Consistent with this hypothesis, shaft polyribosome frequency was correlated with spine synapse density at 5 and 30 min after LTP induction (Figure 3b) and with spine polyribosomes at 5 min (Figure 3c). The correlation between shaft and spine polyribosomes at 5 min after LTP induction was significant for polyribosomes in both spine heads and bases (not shown; shafts vs. heads $r = .697$, $p = .0006$; shafts vs. bases $r = .816$, $p = .00001$). Excitatory shaft synapse frequency was not correlated with shaft or spine polyribosomes (not shown). Thus overall, in the early LTP time points where polyribosomes were upregulated, polyribosomes were associated specifically with synapses on dendritic spines.

3.3 | Multiple polyribosomes accumulated in spines early during LTP

Individual polyribosomes are likely translating a single mRNA, whereas different polyribosomes could be translating different mRNAs. Although most spines had either zero or a single polyribosome, some had more than one (Figure 4a,b). In the 5 min experiment, LTP resulted in more spines containing multiple polyribosomes (Figure 4c), but not more spines with a single polyribosome (Figure 4d). Furthermore, this effect was specific to spines with polyribosomes in more than one of the three defined locations (Figure 4e), as opposed to multiple polyribosomes in a single location (Figure 4f). There were no differences

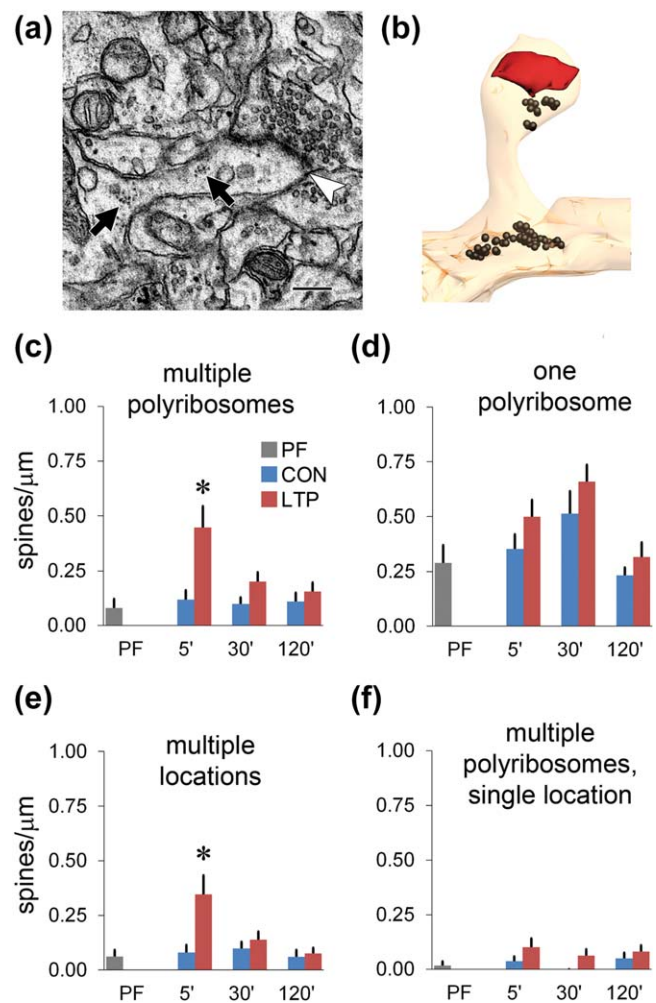


FIGURE 4 Multiple polyribosomes were transiently elevated in multiple locations of individual spines following induction of LTP. (a) EM from the 5 min LTP group with polyribosomes (black arrows) in the base and head of a spine. The white arrowhead indicates the synapse. (b) Reconstruction of the spine in (a) showing its synapse (red) and polyribosomes (black). (c) There were more spines with more than one polyribosome 5 min after LTP induction ($F_{(1, 37)} = 9.66$, $p = .0036$). The differences in spines with only one polyribosome were not significant. (e) Of the spines with multiple polyribosomes, there were more with polyribosomes in multiple locations at 5 min ($F_{(1, 37)} = 7.73$, $p = .0087$). (f) Spines with multiple polyribosomes in a single location were few, and did not differ significantly across time or condition. Effects at $p < .05$: * control versus LTP. Scale in a = 250 nm [Color figure can be viewed at wileyonlinelibrary.com]

between combinations of locations, i.e., base and neck, neck and head (not shown). Regardless of the number of polyribosomes, there were more spines with polyribosomes only in the base for the 30 min LTP condition ($F_{(1,49)} = 10.04$, $p = .0026$) and only in the spine neck in the 120 min LTP condition ($F_{(1,44)} = 8.32$, $p = .0061$) versus the control conditions (not shown). These findings suggest that multiple proteins were being translated throughout individual spines at 5 min, whereas single (or at least fewer) proteins were being translated in spines at 30 or 120 min after the induction of LTP.

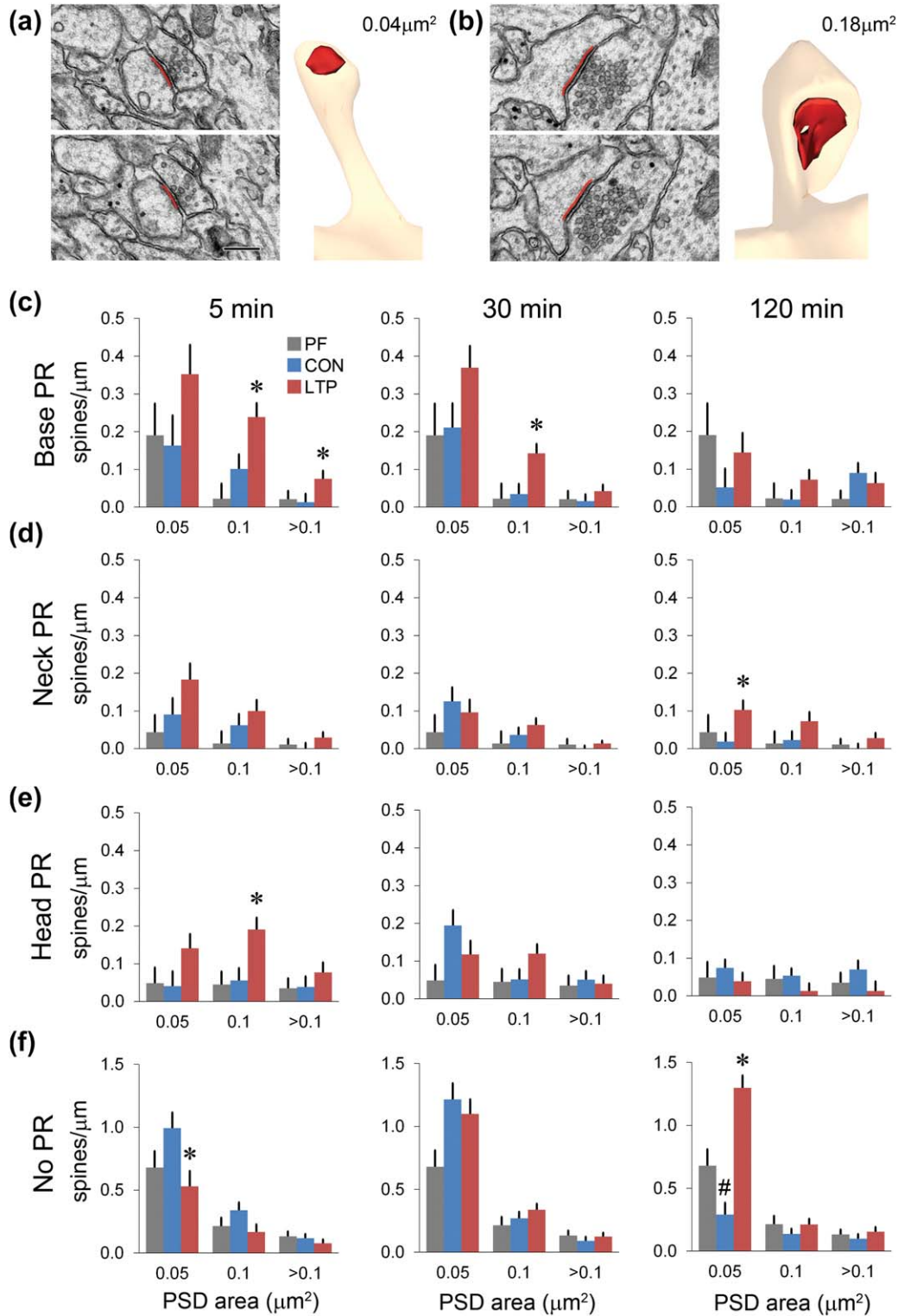


FIGURE 5 Spine density with respect to synapse size and polyribosome location. (a, b) Illustration of PSD measurement approach for cross-sectioned synapses (see Harris et al., 2015 for how the en face and oblique synapse areas were measured). Left panels show EMs of two consecutive sections through a spine from the 30 min LTP condition with the measured length of the PSD on each section in red. Right panels show the reconstructed spine and PSD area. PSD areas are 0.041 μm² and 0.179 μm² in (a) and (b), respectively. (c–f) Spine frequency per micron length of dendrite, binned by PSD area. (c) Among spines with base polyribosomes, there were more with PSD 0.05–0.1 μm² at both 5 min ($F_{(1, 37)} = 5.10, p = .030$) and 30 min ($F_{(1, 49)} = 7.33, p = .0093$), and the 5 and 30 min LTP conditions were not different ($p = .21$). There were more spines with PSD >0.1 μm² ($F_{(1, 37)} = 4.21, p = .047$) at 5 min. (d) For spines with neck polyribosomes, there were more with PSD <0.05 μm² ($F_{(1, 44)} = 5.55, p = .023$) at 120 min. (e) For spines with head polyribosomes, there were more with PSD 0.05–0.1 μm² ($F_{(1, 37)} = 7.46, p = .0096$) at 5 min. (f) For spines with no polyribosomes and PSD <0.05 μm², there were fewer at 5 min ($F_{(1, 37)} = 6.30, p = .017$; LTP × experiment interaction ($F_{(1, 35)} = 12.77, p = .0010$)) and more at 120 min ($F_{(1, 44)} = 56.39, p < .00001$), with fewer in the 120 min control versus perfused ($F_{(1, 39)} = 9.83, p = .0033$). Effects at $p < .05$: * control versus LTP; # control versus perfused. Scale in a, b = 250 nm [Color figure can be viewed at wileyonlinelibrary.com]

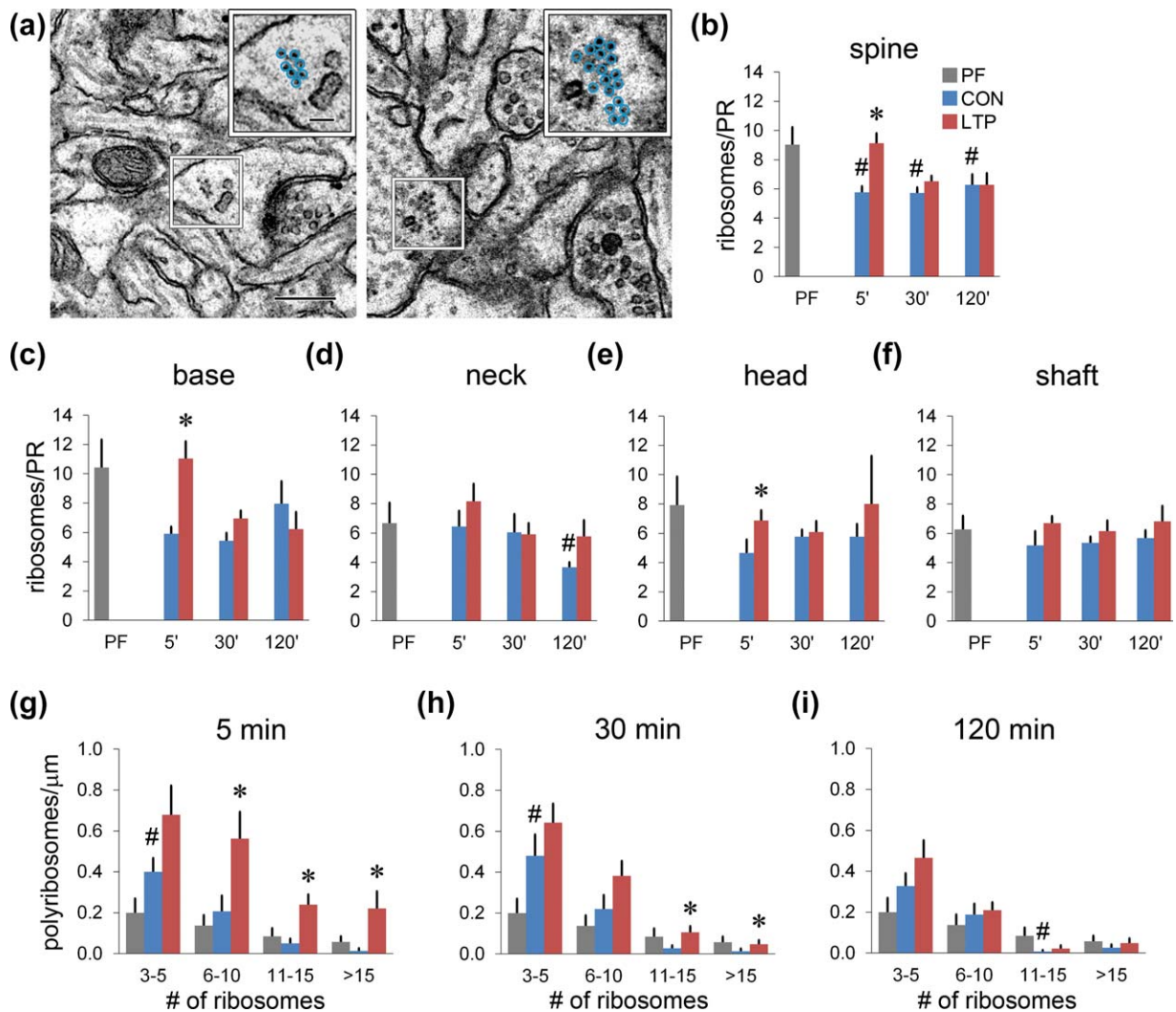


FIGURE 6 Ribosomes per polyribosome. (a) EMs of polyribosomes in a spine head (left) from the 30 min control condition and in a spine base (right) from the 5 min LTP condition. Insets show higher magnification images with individual ribosomes circled in blue. There are seven ribosomes on the left and 18 on the right. (b) There were more ribosomes per polyribosome (PR) in the perfusion fixed (PF) condition versus the control (CON) conditions at 5 min ($F_{(1, 85)} = 8.81$, $p = .0037$), 30 min ($F_{(1, 98)} = 10.43$, $p = .0017$), and 120 min ($F_{(1, 98)} = 6.50$, $p = .013$), and more in the 5 min LTP condition versus control ($F_{(1, 175)} = 11.07$, $p = .0011$). (c) Base polyribosomes were larger (having more ribosomes) after induction of LTP at 5 min ($F_{(1, 85)} = 10.11$, $p = .0021$). (d) Neck polyribosomes were smaller (having fewer ribosomes) in the 120 min control versus perfused ($F_{(1, 8)} = 5.68$, $p = .044$). (e) Head polyribosomes were significantly larger with LTP relative to CON at 5 min ($F_{(1, 50)} = 4.35$, $p = .042$). (f) The size of shaft polyribosomes was unaffected by LTP or control conditions relative to PF. (g–i) Polyribosome frequency binned by number of ribosomes. (g) At 5 min, there were more polyribosomes with 6–10 ($F_{(1, 37)} = 7.87$, $p = .0080$), 11–15 ($F_{(1, 37)} = 10.72$, $p = .0023$), and >15 ribosomes ($F_{(1, 37)} = 5.97$, $p = .019$) in the LTP condition versus control, and more with 3–5 ribosomes in the control versus perfused ($F_{(1, 34)} = 5.23$, $p = .029$). (h) At 30 min, there were more polyribosomes with 11–15 ($F_{(1, 49)} = 4.76$, $p = .034$) and >15 ribosomes ($F_{(1, 49)} = 5.26$, $p = .026$) in the LTP condition versus control, and more with 3–5 ribosomes in the control versus perfused ($F_{(1, 38)} = 6.48$, $p = .015$). (i) At 120 min, there were fewer polyribosomes with 11–15 ribosomes in the control versus perfused ($F_{(1, 37)} = 5.20$, $p = .028$). There were more polyribosomes in the 5 min LTP group versus the 30 min LTP group for 11–15 ribosomes ($p = .014$) and >15 ribosomes ($p = .027$). Effects at $p < .05$: * control versus LTP; # control versus perfused. Scales in a = 250 nm, 100 nm (inset) [Color figure can be viewed at wileyonlinelibrary.com]

3.4 | Polyribosomes accumulated preferentially in spines with larger synapses after the induction of LTP

The spine enlargement that occurs within 5 min of LTP-inducing stimulation requires protein synthesis (Fifkova et al., 1982; Tanaka et al., 2008), and we hypothesized that polyribosomes would accumulate at enlarged spines during the minutes following LTP induction. To test

this hypothesis, we divided the spine population according to postsynaptic density (PSD) areas as small ($PSD < 0.05 \mu\text{m}^2$, Figure 5a), medium (PSD ranging $0.05\text{--}0.10 \mu\text{m}^2$), and large ($PSD > 0.1 \mu\text{m}^2$, Figure 5b).

More spines with medium and large synapses had base polyribosomes after LTP, and this effect reached statistical significance at 5 and 30 min (Figure 5c). Similarly, more small spines had base polyribosomes

at all three time points after LTP, but none of these effects reached statistical significance. More spines of all sizes also tended to accumulate neck polyribosomes, but this effect only reached statistical significance for the small spines at 120 min after LTP (Figure 5d). Among spines with head polyribosomes, there was a significant increase in medium-sized spines at 5 min (Figure 5e), although the means for small and large spines were nonsignificantly higher. Overall, polyribosomes accumulated in spines of all sizes during early LTP, with a bias toward the base and head of larger spines at the earlier time points.

In contrast, changes in spines without polyribosomes occurred only among small spines (Figure 5f). At 5 min, a decrease in small spines without polyribosomes balanced the increase in larger spines with polyribosomes, suggesting a relationship between the presence of spine polyribosomes and synapse growth. By 120 min there was a significant loss of small spines without polyribosomes in the control slice samples versus the perfused material, and a dramatic increase with LTP. Thus, polyribosomes appear to be associated with synapse growth in the early period of LTP, but not with either the elimination after control stimulation, or the outgrowth following LTP of small spines over a longer time course.

3.5 | Polyribosomes were smaller in slices but transiently enlarged during LTP

Translation can be regulated at the initiation, elongation, and termination steps (Costa-Mattioli, Sossin, Klann, & Sonenberg, 2009; Groppo & Richter, 2009). Translational control mechanisms engaged by LTP could affect not only polyribosome number, but size as well. In a previous study of developing hippocampal slices, we found no difference in the number of individual ribosomes per polyribosome 120 min after induction of LTP by tetanic stimulation (Ostroff et al., 2002). However, theta-burst induction of LTP engages multiple mechanisms, and hence might require more refined translation mechanisms. Here, the number of individual ribosomes per polyribosome (i.e., polyribosome size) varied substantially (Figure 6a). Polyribosomes in dendritic shafts and spines had an average of 8 ± 1 ribosomes in the perfused condition, ranging from 3 (our defined minimum) to 38. For polyribosomes in spines, the number of ribosomes was lower in slices in the control than the perfused condition at all three time points, an effect that was reversed by LTP at 5 min only (Figure 6b). Within spines, polyribosomes were larger in both the base and the head in the 5 min LTP versus control conditions (Figure 6c, e). Polyribosomes were smaller in the neck in the 120 min control condition versus perfused, an effect that was reversed by LTP (Figure 6d). The size of shaft polyribosomes was constant across conditions (Figure 6f).

We next wondered whether these results reflected changes in the distribution of polyribosome size as defined by the number of ribosomes in each (Figure 6g–i). In the control versus perfused conditions, we found that the decrease in ribosomes per polyribosome was due to an increase in the frequency of polyribosomes with just 3–5 ribosomes in both the 5 and 30 min experiments (Figure 6g,h), and to a decrease in medium polyribosomes with 11–15 ribosomes at 120 min (Figure 6i). At 5 and 30 min after LTP induction, polyribosomes of all sizes

increased, reaching statistical significance for the 6–10, 11–15, and >15 ribosomes at 5 min and 11–15 and >15 ribosomes at 30 min (Figure 6h). None of these differences remained significant at 120 min after LTP induction (Figure 6i). The distribution of shaft polyribosome size was not different between any of the groups (not shown). In addition, there were no correlations between synapse size and spine polyribosome size at any time or in any location (not shown).

4 | DISCUSSION

Local translation can allow precise spatial and temporal regulation of protein targeting at synapses (Holt & Schuman, 2013; Martin & Ephrussi, 2009), but how this unfolds over the course of LTP consolidation is unclear. Here, we explored the spatiotemporal dynamics of local translation during hippocampal LTP taking advantage of the high resolution and rich detail of serial EM to analyze dendritic polyribosomes. We chose times during and after the initial wave of translation producing proteins that ultimately support later LTP. Our data reveal profound shifts in polyribosome distribution during the first minutes of LTP and suggest that dendritic translation is regulated on a fine spatial scale at specific spine synapses. The effects do not appear to be associated with the LTP-induced synaptogenesis because the new small spines were not observed until the 120 min time point, and typically had no polyribosomes. The nonuniform yet specific changes in the distribution of polyribosomes across time and location suggest some polyribosomes represent sites of active translation, whereas others represent stalled translation in preparation for subsequent plasticity.

In order to stabilize enduring LTP, synapses require new proteins immediately after induction (Otani et al 1989, Frey and Morris 1997). Translation of pre-existing mRNAs in distal dendrites would be an efficient means to supply them and bypass the time needed to transport proteins or mRNAs from the soma. We found a dramatic, widespread increase in shaft and spine polyribosomes at 5 min after LTP induction, followed by a more modest, spatially restricted increase in specific spine locations at 30 and 120 min. Based on what is known about mRNA trafficking in dendrites, it is likely that the additional polyribosomes were translating pre-existing dendritic mRNAs at 5 min. Our tissue was sampled 150–200 μm from the cell body layer. In addition, we excluded large caliber apical dendrites, so the distance between the soma and the synapses we analyzed on thin oblique dendritic branches was likely to be even >200 μm . In cultured hippocampal neurons, newly transcribed radiolabeled RNA travels through dendrites at rates of up to 0.35 $\mu\text{m}/\text{min}$ (Davis, Burger, Banker, & Steward, 1990), and thus would take more than 1 hr to travel from the soma to reach the analyzed synapses. Live imaging studies of cultured neurons have reported rates of $\sim 6 \mu\text{m}/\text{min}$ for RNA granules (Knowles et al., 1996), < 30 $\mu\text{m}/\text{min}$ for the CaMKII α mRNA dendritic targeting element (Rook, Lu, & Kosik, 2000; Tübing et al., 2010), and $\sim 78 \mu\text{m}/\text{min}$ for β -actin mRNA, which is reduced upon stimulation (Buxbaum, Wu, & Singer, 2014; Park et al., 2014). These and other studies report that mRNA moves bidirectionally, is often stationary, and takes relatively short trips. Stimulation can also drive new mRNAs, such as Arc mRNA,

into dendrites, but this process takes more than 30 min (Steward, Wallace, Lyford, & Worley, 1998). Some other mRNAs also undergo stimulation-induced transport; however, these do not include the synaptic molecule CaMKII α , whose dendritic localization is necessary for hippocampal LTP (de Solis, Morales, Hosek, Partin, & Ploski, 2017; Miller et al., 2002). In contrast, under baseline conditions, there are a large variety of mRNAs in hippocampal dendrites (Cajigas et al., 2012; Poon et al., 2006; Zhong et al., 2006). Thus, upon induction of LTP, synapses likely rely on rapid activation of mRNAs constitutively present in dendrites, rather than on transport of new mRNAs and proteins from the soma. Our observations at 30 and 120 min are also consistent with this interpretation. If LTP-associated synapse formation or growth were instead supported by transport of new mRNAs, then the largest increase in polyribosomes should have occurred at the later rather than the earlier times we observed here after induction of LTP.

In addition to supplying proteins rapidly in distal dendrites, local translation could target them on a fine spatial scale. Within dendritic spines, we found that polyribosomes were upregulated transiently in heads but persistently in bases, suggesting differential regulation. There is some evidence that different mRNAs are translated at these locations. Two mRNAs, β -actin and CaMKII α , have been confirmed to localize to spine heads (Kao et al., 2010; Tiruchinapalli et al., 2003). CaMKII α protein accumulates in hippocampal dendrites within 5 min of LTP induction, faster than it can be transported from the soma; furthermore, mGluR1 activation induces translation of CaMKII α mRNA in spine heads, but not dendritic shafts, of cultured hippocampal neurons (Kao et al., 2010; Ouyang, Rosenstein, Kreiman, Schuman, & Kennedy, 1999). This last effect was evident within 5 min and gone within 30 min, consistent with the time course that we observed of polyribosomes in spine heads. Unlike β -actin and CaMKII α mRNAs, Arc and dendrin mRNAs have been reported to localize preferentially to spine bases and proximal necks (Dynes & Steward, 2012). Dendritic translation of Arc in dentate gyrus has a slow onset after synaptic stimulation *in vivo* (Steward et al., 1998), while in cultured CA1 neurons it is translated at spine bases, but not heads, within 5 min of glutamate stimulation (Na et al., 2016). We found upregulated polyribosomes in spine bases at 5, 30, and 120 min, and in spine necks at 120 min, consistent with rapid and sustained Arc translation at these locations. While CaMKII α supports synapse strengthening in LTP (Hell, 2014), Arc is associated with homeostatic reduction of synapse strength, and accumulates in spines that do not expand after LTP-inducing stimulation (Okuno et al., 2012; Rial Verde, Lee-Osbourne, Worley, Malinow, & Cline, 2006; Shepherd et al., 2006). We found that polyribosomes accumulated in larger spine heads at 5 min but in small spine necks at 120 min, consistent with the early, transient translation of CaMKII α in enlarging spines, and the sustained translation of Arc in nonenlarged spines. Larger spines did accumulate base polyribosomes at the earlier time points, so the base location is not purely associated with small spines. There were more spines with polyribosomes in multiple locations at 5 min, so a possible scenario is that enlarging spines transiently accumulate polyribosomes in the head and base, while nonenlarging spines accumulate polyribosomes persistently in the base and neck.

Polyribosomes were also transiently upregulated in dendritic shafts, possibly reflecting the translation of nonsynaptic proteins or a pool of proteins that were available to all synapses. A major characteristic of LTP is associativity, a form of metaplasticity in which LTP at one input facilitates LTP at other inputs, generally within a restricted time window (Abraham, Mason-Parker, Bear, Webb, & Tate, 2001; Malenka, 2003; Reymann & Frey, 2007). In CA1 slices, late LTP can be induced by tetanic stimulation in the presence of a protein synthesis inhibitor if LTP was induced on a second pathway 35 min prior in the absence of inhibitor (Frey & Morris, 1997). This finding suggests that regulation of translation does not need to be contained within spines, but that synapses can share proteins necessary for LTP. Later work demonstrated that this phenomenon is spatially restricted to inputs on the same dendritic branch (Govindarajan et al., 2011; Sajikumar, Navakode, & Frey, 2007). At the level of dendritic segments, we found that the frequency of shaft polyribosomes was correlated with the frequency of spine polyribosomes and spine synapses during the early LTP time points. This finding is consistent with either induction of translation in shafts by local synaptic activity, or with selective trafficking of shaft polyribosomes to activated areas of the dendrite. Previously, we found that polyribosomes were increased in spines and depleted in shafts 120 min after LTP induction by tetanic stimulation, suggestive of capture of shaft polyribosomes by spines (Ostroff et al., 2002). In the present study, we did not observe this shaft to spines redistribution pattern. The most likely explanation for this discrepancy is that here we used TBS, a more naturalistic and effective means of inducing LTP (Larson & Munkácsy, 2015; Larson, Wong, & Lynch, 1986; Nguyen & Kandel, 1997). One study, which used a weaker theta-burst protocol than ours, found that LTP-related proteins could be shared between inputs when a tetanic stimulation was used, but not following TBS (Huang & Kandel, 2005). Thus, we suspect that the polyribosomes we observed in large dendritic spines at 5 min were not captured from the dendritic shafts, as explained by evidence for their differential regulation discussed next.

An unexpected finding in our experiments was the variability in the number of ribosomes per polyribosome, namely, polyribosome size. Like changes in polyribosome number, changes in polyribosome size may reflect differences in translation regulation, the identity of mRNAs, or both. We found that polyribosomes in dendritic spines, but not shafts, were smaller in the slices versus the perfused material, indicating differential regulation between shafts and spines. Spine polyribosomes enlarged transiently in the 5 min LTP condition and were larger than shaft polyribosomes, suggesting they were not derived from the same pool. Translation is regulated at the initiation, elongation, and termination steps, with the initiation step being of particular importance in plasticity and memory (Buffington, Huang, & Costa-Mattioli, 2014; Groppo & Richter, 2009). Very little is known about the factors that affect polyribosome size, but increased initiation, which is well known to occur after LTP induction, could explain the increase we observed. Recent studies have found that ribosome density is not uniform, but differs between and within transcripts, varies inversely with transcript length, and appears to correlate with gene ontology (Andreev et al., 2017; Ciandrini, Stansfield, & Romano, 2013; Ingolia, Ghaemmaghami,

Newman, & Weissman, 2009). Our data could reflect slicing-induced downregulation of a subset of transcripts in spines, and transient, LTP-induced translation of these or other transcripts. The increase in shaft polyribosomes in the 5 min LTP condition was not accompanied by a change in size, thus, these polyribosomes could represent a separate population from those in the spines.

In theory, increased numbers of polyribosomes should result from a combination of upregulated initiation and downregulated elongation and termination, while changes in average polyribosome size could result from altered elongation and termination rates or translation of longer or shorter mRNAs. Upregulated initiation is well established to occur after LTP induction, and could explain the greater number of polyribosomes in our LTP condition (Buffington et al., 2014). Slowed, or even stalled, elongation would also result in more polyribosomes. Once ribosomes are loaded onto mRNA (the initiation step), they can be stalled in place, leaving translation suspended. Stalled polyribosomes can be transported to dendrites from the soma, which can occur in response to activity (Richter & Collier, 2015). Activity could also induce active polyribosomes to stall in dendrites. The dendritically localized protein FMRP, whose action as a translation repressor is central to synaptic plasticity and memory, acts by stalling polyribosomes on certain target mRNAs (Bagni & Oostra, 2013; Darnell et al., 2011). Polyribosomes at spine bases have been shown to be insensitive to puromycin, indicating that they are stalled (Dynes & Steward, 2012), and we have found that polyribosomes in spine bases and necks, but not heads, are insensitive to inhibition of initiation in the lateral amygdala during memory consolidation (Ostroff et al., 2017). The persistent upregulation of polyribosomes that we observed in spine bases and necks may reflect LTP-induced stalling of polyribosomes in nonenlarged spines, while the transient accumulation of enlarged polyribosomes in larger spines could reflect a wave of upregulated initiation and translation of a separate set of mRNAs that support LTP. The upregulated polyribosomes in dendritic shafts were smaller than those in spines at 5 min, but similar in size to those in spine bases and necks at the later time points. Although it is possible that these are stalled polyribosomes, which translocate from shafts to spines, they most likely represent upregulation of nonsynaptic transcripts.

Polyribosome accumulation was not associated with filopodia, shaft synapses, or newly formed spines late after the induction of LTP. In developing hippocampus, filopodia may in fact draw axons to the dendrite and give rise to shaft synapses, rather than being precursors to dendritic spines (Fiala, Feinberg, Popov, & Harris, 1998; Harris, 1999; Marrs, Green, & Dailey, 2001). The initial accumulation of polyribosomes in spine heads and bases was not sustained with the proliferation of small spines at 120 min after induction of LTP. In adult hippocampus, theta-burst LTP results in the enlargement of synapses on spines with polyribosomes, which is balanced by failure to form, or elimination of, small spines (Bell et al., 2014; Bourne & Harris, 2011). Synaptic responses were not further increased at 120 min following induction of LTP, beyond that observed at 5 or 30 min, in either developing or adult hippocampus. Thus, the new small synapses are likely to be silent in the developing hippocampus and following control stimulation in the adults. Furthermore, the PSD enlargement in adults was

achieved primarily by the addition of silent nascent zones, regions at the edges of the enlarged PSDs without presynaptic vesicles (Bell et al., 2014). Thus, as in the adult, polyribosomes were associated with LTP-related PSD enlargement during development, but not with the addition of new silent synapses. If the later accumulation of polyribosomes were instead stalled in the base or neck of newly formed or silent synapses, then they could be there in reserve to engage those synapses during subsequent plasticity. Overall, our results corroborate a specific role for local translation in providing a rapid supply of new proteins to support and strengthen existing spine synapses that have undergone LTP.

ACKNOWLEDGMENTS

We thank Libby Perry, Robert Smith, and John Mendenhall for technical assistance with the electron microscopy. LEO and KMH designed the experiments; LEO and GC performed the slice electrophysiology; LEO and GC prepared samples and collected images; DJW, LEO, PHP, HS, and KMH completed the 3D reconstructions; LEO and KMH performed the statistical analyses and wrote the paper. All co-authors provided editorial input. We thank members of the Harris Laboratory for insightful discussions. This work was funded by NIH grants NS201184, MH095980, and NS074644 and NSF NeuroNex 1707356 to KMH and MH096459 to DJW, and the Texas Emerging Technologies Fund.

CONFLICTS OF INTEREST

The authors declare no financial conflicts of interest.

ORCID

Linnaea E. Ostroff  <http://orcid.org/0000-0002-3348-342X>

REFERENCES

- Abraham, W. C., Mason-Parker, S. E., Bear, M. F., Webb, S., & Tate, W. P. (2001). Heterosynaptic metaplasticity in the hippocampus in vivo: A BCM-like modifiable threshold for LTP. *Proceedings of the National Academy of Sciences of the United States of America*, *98*(19), 10924–10929.
- Abraham, W. C., & Williams, J. M. (2008). LTP maintenance and its protein synthesis-dependence. *Neurobiology of Learning and Memory*, *89*(3), 260–268.
- Alberini, C. M. (2008). The role of protein synthesis during the labile phases of memory: revisiting the skepticism. *Neurobiology of Learning and Memory*, *89*(3), 234–246.
- Andreev, D. E., O'Connor, P. B. F., Loughran, G. A., Dmitriev, S. E., Baranov, P. V., & Shatsky, I. N. (2017). Insights into the mechanisms of eukaryotic translation gained with ribosome profiling. *Nucleic Acids Research*, *45*(2), 513–526.
- Bagni, C., & Oostra, B. A. (2013). Fragile X syndrome: From protein function to therapy. *American Journal of Medical Genetics Part A*, *161*(11), 2809–2821.
- Bell, M. E., Bourne, J. N., Chirillo, M. A., Mendenhall, J. M., Kuwajima, M., & Harris, K. M. (2014). Dynamics of nascent and active zone ultrastructure as synapses enlarge during long-term potentiation in mature hippocampus. *Journal of Comparative Neurology*, *522*(17), 3861–3884.

- Bourne, J. N., & Harris, K. M. (2011). Coordination of size and number of excitatory and inhibitory synapses results in a balanced structural plasticity along mature hippocampal CA1 dendrites during LTP. *Hippocampus*, 21(4), 354–373.
- Bradshaw, K. D., Emptage, N. J., & Bliss, T. V. (2003). A role for dendritic protein synthesis in hippocampal late LTP. *The European Journal of Neuroscience*, 18(11), 3150–3152.
- Buffington, S. A., Huang, W., & Costa-Mattioli, M. (2014). Translational control in synaptic plasticity and cognitive dysfunction. *Annual Review of Neuroscience*, 37(1), 17–38.
- Buxbaum, A. R., Wu, B., & Singer, R. H. (2014). Single β -actin mRNA detection in neurons reveals a mechanism for regulating its translatability. *Science*, 343(6169), 419–422.
- Cajigas, I. J., Tushev, G., Will, T. J., Tom Dieck, S., Fuerst, N., & Schuman, E. M. (2012). The local transcriptome in the synaptic neuropil revealed by deep sequencing and high-resolution imaging. *Neuron*, 74(3), 453–466.
- Cao, G., & Harris, K. M. (2012). Developmental regulation of the late phase of long-term potentiation (L-LTP) and metaplasticity in hippocampal area CA1 of the rat. *Journal of Neurophysiology*, 107(3), 902–912.
- Chen, P. B., Kawaguchi, R. I., Blum, C. H., Achiro, J. M., Coppola, G. I., O'Dell, T. J., & Martin, K. C. (2017). Mapping gene expression in excitatory neurons during hippocampal late-phase long-term potentiation. *Frontiers in Molecular Neuroscience*, 10, 39.
- Ciandrini, L., Stansfield, I., & Romano, M. C. (2013). Ribosome traffic on mRNAs maps to gene ontology: Genome-wide quantification of translation initiation rates and polysome size regulation. *PLoS Computational Biology*, 9(1), e1002866.
- Costa-Mattioli, M., Gobert, D., Stern, E., Gamache, K., Colina, R., Cuello, C., ... Sonenberg, N. (2007). eIF2 α phosphorylation bidirectionally regulates the switch from short- to long-term synaptic plasticity and memory. *Cell*, 129(1), 195–206.
- Costa-Mattioli, M., Sossin, W. S., Klann, E., & Sonenberg, N. (2009). Translational control of long-lasting synaptic plasticity and memory. *Neuron*, 61(1), 10–26.
- Cracco, J. B., Serrano, P., Moskowitz, S. I., Bergold, P. J., & Sacktor, T. C. (2005). Protein synthesis-dependent LTP in isolated dendrites of CA1 pyramidal cells. *Hippocampus*, 15(5), 551–556.
- Darnell, J. C., Van Driesche, S. J., Zhang, C., Hung, K. Y. S., Mele, A., Fraser, C. E., ... Darnell, R. B. (2011). FMRP stalls ribosomal translocation on mRNAs linked to synaptic function and autism. *Cell*, 146(2), 247–261.
- Davis, L., Burger, B., Banker, G., & Steward, O. (1990). Dendritic transport: Quantitative analysis of the time course of somatodendritic transport of recently synthesized RNA. *Journal of Neuroscience*, 10, 3056–3068.
- Davis, H. P., & Squire, L. R. (1984). Protein synthesis and memory: A review. *Psychological Bulletin*, 96(3), 518–559.
- de Solis, C. A., Morales, A. A., Hosek, M. P., Partin, A. C., & Ploski, J. E. (2017). Is Arc mRNA unique: A search for mRNAs that localize to the distal dendrites of dentate gyrus granule cells following neural activity. *Frontiers in Molecular Neuroscience*, 10, 314.
- Dynes, J. L., & Steward, O. (2012). Arc mRNA docks precisely at the base of individual dendritic spines indicating the existence of a specialized microdomain for synapse-specific mRNA translation. *The Journal of Comparative Neurology*, 520(14), 3105–3119.
- Engert, F., & Bonhoeffer, T. (1999). Dendritic spine changes associated with hippocampal long-term synaptic plasticity. *Nature*, 399(6731), 66–70.
- Fiala, J. C. (2005). Reconstruct: A free editor for serial section microscopy. *Journal of Microscopy*, 218(Pt 1), 52–61.
- Fiala, J. C., Feinberg, M., Popov, V., & Harris, K. M. (1998). Synaptogenesis via dendritic filopodia in developing hippocampal area CA1. *The Journal of Neuroscience: The Official Journal of the Society for Neuroscience*, 18(21), 8900–8911.
- Fiala, J. C., & Harris, K. M. (2001). Extending unbiased stereology of brain ultrastructure to three-dimensional volumes. *Journal of the American Medical Informatics Association*, 8(1), 1–16.
- Fiala, J. C., Kirov, S. A., Feinberg, M. D., Petrak, L. J., George, P., Goddard, C. A., & Harris, K. M. (2003). Timing of neuronal and glial ultrastructure disruption during brain slice preparation and recovery in vitro. *The Journal of Comparative Neurology*, 465(1), 90–103.
- Fifkova, E., Anderson, C. L., Young, S. J., & Van Harrevelde, A. (1982). Effect of anisomycin on stimulation-induced changes in dendritic spines of the dentate granule cells. *Journal of Neurocytology*, 11(2), 183–210.
- Frey, U., Krug, M., Reymann, K. G., & Matthies, H. (1988). Anisomycin, an inhibitor of protein synthesis, blocks late phases of LTP phenomena in the hippocampal CA1 region in vitro. *Brain Research*, 452(1–2), 57–65.
- Frey, U., & Morris, R. G. (1997). Synaptic tagging and long-term potentiation. *Nature*, 385(6616), 533–536.
- Govindarajan, A., Israely, I., Huang, S.-Y., & Tonegawa, S. (2011). The dendritic branch is the preferred integrative unit for protein synthesis-dependent LTP. *Neuron*, 69(1), 132–146.
- Groppo, R., & Richter, J. D. (2009). Translational control from head to tail. *Current Opinion in Cell Biology*, 21(3), 444–451.
- Harris, K. M. (1999). Structure, development, and plasticity of dendritic spines. *Current Opinion in Neurobiology*, 9(3), 343–348.
- Harris, K. M., Spacek, J., Bell, M. E., Parker, P. H., Lindsey, L. F., Baden, A. D., ... Burns, R. (2015). A resource from 3D electron microscopy of hippocampal neuropil for user training and tool development. *Scientific Data*, 2, 150046.
- Hell, J. W. (2014). CaMKII: claiming center stage in postsynaptic function and organization. *Neuron*, 81(2), 249–265.
- Hirokawa, N., & Takemura, R. (2005). Molecular motors and mechanisms of directional transport in neurons. *Nature Reviews. Neuroscience*, 6(3), 201–214.
- Holt, C. E., & Schuman, E. M. (2013). The central dogma decentralized: New perspectives on RNA function and local translation in neurons. *Neuron*, 80(3), 648–657.
- Huang, Y.-Y., & Kandel, E. R. (2005). Theta frequency stimulation induces a local form of late phase LTP in the CA1 region of the hippocampus. *Learning & Memory*, 12(6), 587–593.
- Ingolia, N. T., Ghaemmaghami, S., Newman, J. R. S., & Weissman, J. S. (2009). Genome-wide analysis in vivo of translation with nucleotide resolution using ribosome profiling. *Science*, 324(5924), 218–223.
- Kang, H., & Schuman, E. M. (1996). A requirement for local protein synthesis in neurotrophin-induced hippocampal synaptic plasticity. *Science*, 273(5280), 1402–1406.
- Kao, D.-I., Aldridge, G. M., Weiler, I. J., & Greenough, W. T. (2010). Altered mRNA transport, docking, and protein translation in neurons lacking fragile X mental retardation protein. *Proceedings of the National Academy of Sciences of the United States of America*, 107(35), 15601–15606.
- Kapitein, L. C., Schlager, M. A., Kuijpers, M., Wulf, P. S., van Spronsen, M., MacKintosh, F. C., & Hoogenraad, C. C. (2010). Mixed

- microtubules steer dynein-driven cargo transport into dendrites. *Current Biology*, 20(4), 290–299.
- Kelleher, R. J., Govindarajan, A., & Tonegawa, S. (2004). Translational regulatory mechanisms in persistent forms of synaptic plasticity. *Neuron*, 44(1), 59–73.
- Knowles, R. B., Sabry, J. H., Martone, M. E., Deerinck, T. J., Ellisman, M. H., Bassell, G. J., & Kosik, K. S. (1996). Translocation of RNA granules in living neurons. *The Journal of Neuroscience: The Official Journal of the Society for Neuroscience*, 16(24), 7812–7820.
- Krug, M., Lössner, B., & Ott, T. (1984). Anisomycin blocks the late phase of long-term potentiation in the dentate gyrus of freely moving rats. *Brain Research Bulletin*, 13(1), 39–42.
- Larson, J., & Munkácsy, E. (2015). Theta-burst LTP. *Brain Research*, 1621, 38–50.
- Larson, J., Wong, D., & Lynch, G. (1986). Patterned stimulation at the theta frequency is optimal for the induction of hippocampal long-term potentiation. *Brain Research*, 368(2), 347–350.
- Maeder, C. I., Shen, K., & Hoogenraad, C. C. (2014). Axon and dendritic trafficking. *Current Opinion in Neurobiology*, 27, 165–170.
- Malenka, R. C. (2003). The long-term potential of LTP. *Nature Reviews Neuroscience*, 4(11), 923–926.
- Marrs, G. S., Green, S. H., & Dailey, M. E. (2001). Rapid formation and remodeling of postsynaptic densities in developing dendrites. *Nature Neuroscience*, 4(10), 1006–1013.
- Martin, K. C., & Ephrussi, A. (2009). mRNA localization: Gene expression in the spatial dimension. *Cell*, 136(4), 719–730.
- Matsuzaki, M., Honkura, N., Ellis-Davies, G. C., & Kasai, H. (2004). Structural basis of long-term potentiation in single dendritic spines. *Nature*, 429(6993), 761–766.
- McNamara, J. O., Grigston, J. C., VanDongen, H. M., & VanDongen, A. M. (2004). Rapid dendritic transport of TGN38, a putative cargo receptor. *Molecular Brain Research*, 127(1–2), 68–78.
- Miller, S., Yasuda, M., Coats, J. K., Jones, Y., Martone, M. E., & Mayford, M. (2002). Disruption of dendritic translation of CaMKII α impairs stabilization of synaptic plasticity and memory consolidation. *Neuron*, 36(3), 507–519.
- Na, Y., Park, S., Lee, C., Kim, D.-K., Park, J. M., Sockanathan, S., ... Worley, P. F. (2016). Real-time imaging reveals properties of glutamate-induced Arc/Arg 3.1 translation in neuronal dendrites. *Neuron*, 91(3), 561–573.
- Nguyen, P. V., & Kandel, E. R. (1997). Brief theta-burst stimulation induces a transcription-dependent late phase of LTP requiring cAMP in area CA1 of the mouse hippocampus. *Learning & Memory*, 4(2), 230–243.
- Okuno, H., Akashi, K., Ishii, Y., Yagishita-Kyo, N., Suzuki, K., Nonaka, M., ... Bito, H. (2012). Inverse synaptic tagging of inactive synapses via dynamic interaction of Arc/Arg3.1 with CaMKII β . *Cell*, 149(4), 886–898.
- Ostroff, L. E., Botsford, B., Gindina, S., Cowansage, K. K., LeDoux, J. E., Klann, E., & Hoeffler, C. (2017). Accumulation of polyribosomes in dendritic spine heads, but not bases and necks, during memory consolidation depends on Cap-dependent translation initiation. *The Journal of Neuroscience*, 37(7), 1862–1872.
- Ostroff, L. E., Cain, C. K., Bedont, J., Monfils, M. H., & LeDoux, J. E. (2010). Fear and safety learning differentially affect synapse size and dendritic translation in the lateral amygdala. *Proceedings of the National Academy of Sciences of the United States of America*, 107(20), 9418.
- Ostroff, L. E., Fiala, J. C., Allwardt, B., & Harris, K. M. (2002). Polyribosomes redistribute from dendritic shafts into spines with enlarged synapses during LTP in developing rat hippocampal slices. *Neuron*, 35(3), 535.
- Otani, S., Marshall, C. J., Tate, W. P., Goddard, G. V., & Abraham, W. C. (1989). Maintenance of long-term potentiation in rat dentate gyrus requires protein synthesis but not messenger RNA synthesis immediately post-tetanzation. *Neuroscience*, 28(3), 519–526.
- Ouyang, Y., Rosenstein, A., Kreiman, G., Schuman, E. M., & Kennedy, M. B. (1999). Tetanic stimulation leads to increased accumulation of Ca²⁺/calmodulin-dependent protein kinase II via dendritic protein synthesis in hippocampal neurons. *Journal of Neuroscience*, 19, 7823–7833.
- Park, H. Y., Lim, H., Yoon, Y. J., Follenzi, A., Nwokafor, C., Lopez-Jones, M., ... Singer, R. H. (2014). Visualization of dynamics of single endogenous mRNA labeled in live mouse. *Science*, 343(6169), 422–424.
- Peters, A., Palay, S., & Webster, H. (1991). *The fine structure of the nervous system* (3rd ed.). New York: Oxford University Press.
- Poon, M. M., Choi, S.-H., Jamieson, C. A. M., Geschwind, D. H., & Martin, K. C. (2006). Identification of process-localized mRNAs from cultured rodent hippocampal neurons. *Journal of Neuroscience*, 26(51), 13390–13399.
- Reymann, K. G., & Frey, J. U. (2007). The late maintenance of hippocampal LTP: Requirements, phases, “synaptic tagging”, “late-associativity” and implications. *Neuropharmacology*, 52(1), 24–40.
- Rial Verde, E. M., Lee-Osbourne, J., Worley, P. F., Malinow, R., & Cline, H. T. (2006). Increased expression of the immediate-early gene Arc/Arg3.1 reduces AMPA receptor-mediated synaptic transmission. *Neuron*, 52(3), 461–474.
- Richter, J. D., & Collier, J. (2015). Pausing on polyribosomes: Make way for elongation in translational control. *Cell*, 163(2), 292–300.
- Rook, M. S., Lu, M., & Kosik, K. S. (2000). CaMKII α 3' untranslated region-directed mRNA translocation in living neurons: Visualization by GFP linkage. *Journal of Neuroscience*, 20, 6385–6393.
- Routh, B. N., Johnston, D., Harris, K., & Chitwood, R. A. (2009). Anatomical and electrophysiological comparison of CA1 pyramidal neurons of the rat and mouse. *Journal of Neurophysiology*, 102(4), 2288–2302.
- Sajikumar, S., Navakkode, S., & Frey, J. U. (2007). Identification of compartment- and process-specific molecules required for “synaptic tagging” during long-term potentiation and long-term depression in hippocampal CA1. *Journal of Neuroscience*, 27(19), 5068–5080.
- Segal, M. (2016). Dendritic spines: Morphological building blocks of memory. *Neurobiology of Learning and Memory*, 138, 3–9.
- Shepherd, J. D., Rumbaugh, G., Wu, J., Chowdhury, S., Plath, N., Kuhl, D., ... Worley, P. F. (2006). Arc/Arg3.1 mediates homeostatic synaptic scaling of AMPA receptors. *Neuron*, 52(3), 475–484.
- Stanton, P. K., & Sarvey, J. M. (1984). Blockade of long-term potentiation in rat hippocampal CA1 region by inhibitors of protein synthesis. *The Journal of Neuroscience: The Official Journal of the Society for Neuroscience*, 4(12), 3080–3088.
- Steward, O., & Levy, W. (1982). Preferential localization of polyribosomes under the base of dendritic spines in granule cells of the dentate gyrus. *Journal of Neuroscience*, 2(3), 284–291.
- Steward, O., Wallace, C. S., Lyford, G. L., & Worley, P. F. (1998). Synaptic activation causes the mRNA for the IEG Arc to localize selectively near activated postsynaptic sites on dendrites. *Neuron*, 21(4), 741–751.
- Tanaka, J., Horiike, Y., Matsuzaki, M., Miyazaki, T., Ellis-Davies, G. C., & Kasai, H. (2008). Protein synthesis and neurotrophin-dependent structural plasticity of single dendritic spines. *Science*, 319(5870), 1683–1687.
- Tiruchinapalli, D. M., Oleynikov, Y., Kelic, S., Shenoy, S. M., Hartley, A., Stanton, P. K., ... Bassell, G. J. (2003). Activity-dependent trafficking

- and dynamic localization of zipcode binding protein 1 and beta-actin mRNA in dendrites and spines of hippocampal neurons. *Journal of Neuroscience*, 23, 3251–3261.
- Tübing, F., Vendra, G., Mikl, M., Macchi, P., Thomas, S., & Kiebler, M. A. (2010). Dendritically localized transcripts are sorted into distinct ribonucleoprotein particles that display fast directional motility along dendrites of hippocampal neurons. *Journal of Neuroscience*, 30(11), 4160.
- Vickers, C. A., Dickson, K. S., & Wyllie, D. J. A. (2005). Induction and maintenance of late-phase long-term potentiation in isolated dendrites of rat hippocampal CA1 pyramidal neurones. *The Journal of Physiology*, 568(3), 803–813.
- Warner, J. R., Rich, A., & Hall, C. E. (1962). Electron microscope studies of ribosomal clusters synthesizing hemoglobin. *Science*, 138(3548), 1399–1403.
- Watson, D. J., Ostroff, L., Cao, G., Parker, P. H., Smith, H., & Harris, K. M. (2016). LTP enhances synaptogenesis in the developing hippocampus. *Hippocampus*, 26(5), 560–576.
- Zhong, J., Zhang, T., & Bloch, L. M. (2006). Dendritic mRNAs encode diversified functionalities in hippocampal pyramidal neurons. *BMC Neuroscience*, 7, 17.

How to cite this article: Ostroff LE, Watson DJ, Cao G, Parker PH, Smith H, Harris KM. Shifting patterns of polyribosome accumulation at synapses over the course of hippocampal long-term potentiation. *Hippocampus*. 2018;28:416–430. <https://doi.org/10.1002/hipo.22841>